Sensors & Transducers, Vol. 192, Issue 9, September 2015, pp. 1-8

Sensors & Transducers

http://www.sensorsportal.com

Duty-Cycle and Duty-off Factor Measurements Based on Universal Sensors and Transducers Interface (USTI-MOB) IC

*** Sergey Y. YURISH and Javier CAÑETE**
Excelera, S. L., Parc UPC-PMT, Edificio RDIT-K2M,
c/ Esteve Terradas, 1, 08860, Castelldefels, Barcelona, Spain
Tel.: +34 93 4137941
E-mail: sergey.yurish@excelera.io, javier.canete@excelera.io,

Received: 15 July 2015 /Accepted: 31 August 2015 /Published: 30 September 2015

Abstract: An experimental investigation of metrological characteristics of designed Universal Sensors and Transducers Interface (USTI-MOB) integrated circuit working in duty-cycle and duty-off factor measuring modes is described in the article. The USTI-MOB is based on the novel patented methods for duty-cycle – to – digital conversion. Experiments have confirmed the high metrological performance at low power consumption (0.35 mA current consumption at V_{cc} = 1.8 V). So, the relative error of duty-cycle – to – code conversion is changed from ±0.08 to ±1.00 % in all specified measuring range of USTI-MOB. Metrological characteristics and functionality make the USTI-MOB very suitable for various sensor systems designs, based on duty-cycle output sensors. In this case the significant time-to-marked reduction and design simplification can be achieved.

Keywords: Universal Sensors and Transducers Interface, USTI-MOB, Duty-cycle measurement, Duty-off factor.

1. Introduction

The duty cycle (D.C.) is the ratio between the pulse duration t_p and the period T_x of a rectangular waveform (Fig. 1):

$$D.C. = \frac{t_p}{T_x} \times 100\ \% \qquad (1)$$

The physical meaning of duty-cycle is the percentage of one period in which a signal is active. The value, reciprocal to the duty cycle is called 'duty-off factor':

$$K_{off} = \frac{1}{D.C.} = \frac{T_x}{t_p} \qquad (2)$$

Sometimes the duty-off factor is called 'period-to-pulse duration ratio' or 'relative pulse duration'. Several sensors' and microcontrollers' manufacturers mistakenly use the "duty-cycle output" term instead of "pulse-width modulated (PWM) output". In the last one, the information parameter is a ratio between pulse width t_p and pulse space t_s (t_p/t_s or t_s/t_p) but not the ratio between period T_x and t_p as for the duty-cycle (1). The difference between duty-cycle and PWM informative parameters are shown in Fig. 1.

The duty-cycle of pulse signal (D.C.) is widely used as informative parameter of sensors' outputs and in various measuring and DAQ systems. For example, accelerometers from *Analog Devices*, *Kionix* and *MEMSIC*; temperature sensors from *Smartec* (The Netherlands), magnetic field Hall effect sensor HAL810 from *Micronas*, Hall Effect Differential Gear Tooth Sensors CYGTS101DC-S

from *ChenYang-Technologies GmbH & Co. KG*, and others [1-6]. The duty cycle of the output signal in such sensors is related to the measurand, the measuring value can be easily computed by means of measuring a duty cycle. In comparison with an analog sensor output signal and even with frequency sensor output signal, the duty-cycle is rather immune to interfering signals, such as spikes [7], and the ratio does not depend on the absolute value of any component [8].

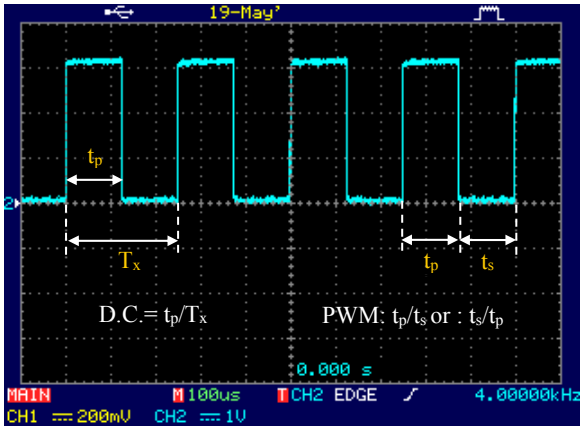

Fig. 1. Difference between duty-cycle and PWM informative parameters.

The D.C. as an informative parameter are also used in different interfacing and readout circuits. So, in the ASIC front-end interface for resistive-bridge sensors based on a relaxation oscillator with frequency and duty cycle output, the D.C. depends on the overall bridge resistance and used as an informative parameter related to the sensor temperature [9].

A capacitive sensor readout circuit that converts capacitance changes of a sensor element to changes of the duty-cycle of a square-wave oscillator is described in [10]. It has achieved a performance of 13-bit effective resolution with a 1-kHz bandwidth. A low-voltage CMOS on-chip design of such readout circuit may also create opportunities for a low-power consumption of the readout circuit [10]. Due to its simplicity and low number of components, the power consumption of the circuit is expected to be significantly smaller than in similar tradition analog readout designs [10].

The designed by authors Universal Sensors and Transducers Interface (USTI-MOB) IC for low power consumption applications contains appropriate measuring modes for duty-cycle, duty-off factor and PWM parameters (pulse width and pulse space) [11].

The aim of this research was to determine the metrological characteristics of designed USTI-MOB at duty-cycle and duty-off factor measurements. The article is organized as follow. In Section I the method for duty-cycle and duty-off factor measurements are described in short. The experimental set-up for duty-cycle and duty-off factor is described in Section II. The obtained experimental results of measurements are provided and discussed in Section III. The Section IV describes two cases of study: an example of temperature sensor system based on duty-cycle output temperature sensors SMT16030, SMT172 (*Smartec*); and accelerometer sensor system. The article is concluded in the last section.

2. Method for Duty-Cycle and Duty-off Factor Measurements

Various methods exist to measure the duty-cycle of pulse signal. For example, some simple duty-cycle - to - digital can be based on the classical approach: to measure the pulse width t_p and period T_x of signal, then calculate the ratio according to equation (1) and (2). Main error's components are quantization errors at pulse width and period measurements. Both components can be big enough. If a high accuracy is needed, a very high clock frequency should be used. For example, the approaches described in [12] and [13] are based on the 33 MHz MCS-51 and 16 MHz Microchip types of microcontrollers. Such high clock frequencies are not suitable for applications with the low power consumption, including mobile devices (smart phones and tablets) and IoT.

Another approach to measure a duty-cycle is to take random samples of a digital signal (random-sampling method) [14]. The method can be realized very easy by a program-oriented way. But this method is suitable only for low-resolution conversions for which the necessary resolution is a maximum of 9 bits.

The method of reading the time-domain sensor signals is described in [15]. It can eliminate the part of quantization error without increase of clock frequency. The method uses the internal clock frequency as 2N times of the signal frequency. So, it means that the period T_x is not changed with the sensor output signal. However, very often, the frequency (period) of signal is changing. In this case this method cannot be used.

The Vernier-type method for duty-cycle measurement is described in [16]. The method using two phase-locked loops (PLLs), developed to emulate the Vernier caliper to measure the duty cycle. The method lets to minimize the measuring error and obtain a higher resolution without increasing the clock frequency. But the main unit - the Vernier Caliper Emulator (VCE), needs two different clock frequencies. Such block has a relatively high power consumption. In addition, the VCE must be calibrated by a calibration signal with a known duty cycle and frequency [16].

Sometime, duty-cycle output sensors' manufactures recommend to convert duty-cycle in voltage, and then, voltage-to-digital by an ADC [17]. Such solution introduces addition component of error due to these two-stage conversion. This error is much

bigger in comparison with the error, which can be achieved at direct duty-cycle – to – digital conversion.

The USTI-MOB is based on novel, patented method for duty-cycle and duty-off factor measurement. The method is based on the determination of average pulse width and average period during the conversion time T_q. The last one is determined by the beforehand given quantization error δ for period measurement and equals to the integer number of periods NT_x. During this time and each of pulse widths, the pulses of the reference frequency are counted. At the end of conversion time the duty cycle is calculated according to the following equation:

$$D.C. = \frac{N_{\bar{T}_x}}{N_{\bar{x}}} = \frac{\bar{t}_p}{\bar{T}_x} \tag{3}$$

and duty-off factor is calculated according to the formula:

$$K_{off} = \frac{N_{\bar{T}x}}{N_{\bar{t}_p}} = \frac{\bar{T}_x}{\bar{t}_p} \tag{4}$$

The duty-cycle (and duty-off factor) measurement contains two main components of error: the error due to period and error due to pulse width measurements. The first one can be eliminated due to the described above method for the duty-cycle measurement, which is used in the USTI-MOB. The second component (relative quantization error) can be calculated in the worst case (one period T_x) according to the following equation:

$$\delta_q = \frac{1}{4\times10^6 \times t_p} \times 100\,\% \tag{5}$$

3. Measurement Technique and Experimental Set-Up

The diagram of experimental measurement set-up for the USTI-MOB working in duty cycle and duty-off factor measuring modes is the same as it is shown in [18]. The circuit diagram is similar to the USTI circuit diagram of connection [19]. The difference is only in the voltage of power supply V_{cc}: +1.8 V for the USTI-MOB and +5 V for the USTI.

A square waveform pulse signal whose duty-cycle and duty-off factor must be measured, was fed from the first channel of Waveform Generator Agilent 33500B to inputs FX1, ST1 and FX2, ST2 (the 1st channel of IC) of the USTI-MOB running on a 4 MHz clock.

The supply voltage of the evaluation board was +14 V dc, provided by the Promax FA-851 power supply. The duty-cycle and duty-off factor of signals generated by the waveform generator were measured by both: the USTI-MOB and Universal Frequency Counter/Timer Agilent 53220A with the ultra high oven stability internal time base. The digital oscilloscope Promax OD-591 monitored the signal's waveforms. Before measurements, the USTI-MOB was calibrated in the working temperature range: +24.4 °C at 45-47 % RH. The measurands were sent to a PC via an RS232 interface implemented with the ST202D IC. The user interface was realized with the help of terminal software Terminal V1.9b running under Windows XP or Windows 7 operation systems. The commands of RS232 communication mode for duty-cycle measurements in the 1st USTI-MOB channel are shown in Fig. 2.

M04 ; Select phase shift measurement mode
S ; Start measurement
C ; Check result status: ‘r’ if ready or ‘b if busy
R ; Get result in BCD ASCII format

Fig. 2. Commands for RS232 communication modes at duty-cycle measurements.

In case of duty-off factor measurement mode the first command must be changed to 'M05'. The duty-cycle and duty-off factor can be measured also in the 2nd USTI-MOB channel. It this case it is necessary to use commands 'M14' or 'M15' respectively.

Every measurement were consisted of 60 values (sample size). The measurement errors were evaluated from appropriate statistics with the help of NUMERI software [20].

The Waveform Generator Agilent 33500B has the high-stability OCXO timebase (frequency reference ±0.1 ppm of setting ±15 pHz) [21]. The Universal Frequency Counter/Timer Agilent 53220A-010 has the ultra high-stability OCXO timebase (±50 ppb) [22].

4. Experimental Results

The D.C. range of measurements is dependent on the frequency of input signal. The maximal possible signal frequency for the D.C. measurement by the USTI-MOB is 100 kHz, and duty-cycle can be measured in the narrow range D.C. ~50 %. At 500 Hz frequency, the D.C. can be measured in the wide range from 1 to 99 %. The possible duty-cycle values vs. frequencies are shown in Table 1.

In the experimental investigation, 50 % D.C. was measured at 500 Hz and 100 kHz of input signal 60 times each. The conventional true value for duty-cycle measurement (*D.C.*=50 %) is shown in Fig. 2.

Table 1. Duty-cycle values vs. frequencies.

Frequency, kHz	Duty-cycle, %
< 0.5	1 ... 99.3
1	1.5 ... 98
10	15 ... 80
20	30 ... 71
30	46 ... 60
> 40	50

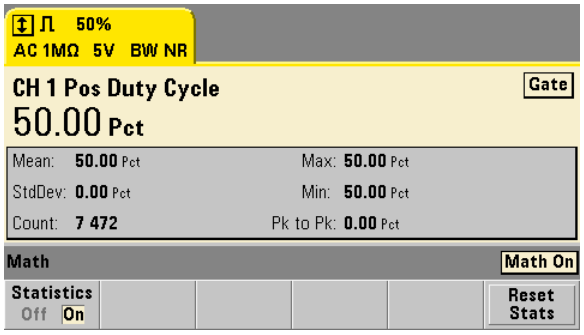

Fig. 2. Conventional true value for duty-cycle measurement (*D.C.* = 50 % at 500 Hz).

The experimental results of duty-cycle measurements are shown in Fig.3-5, and statistical characteristics - in Table 2.

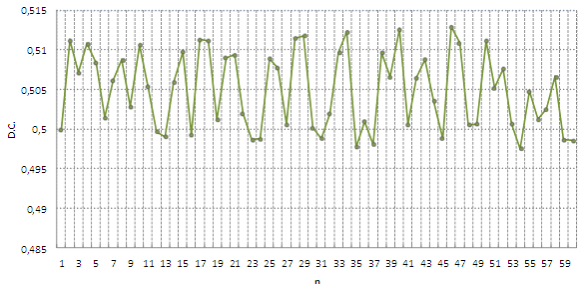

Fig. 3. Results of measurements for duty-cycle of 100 kHz input signal.

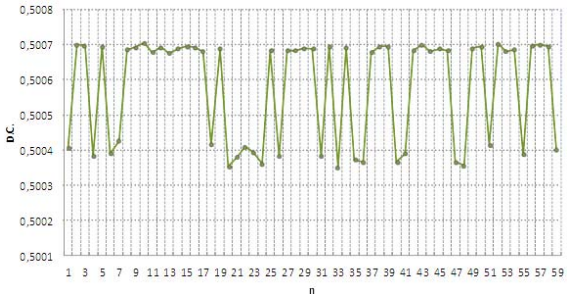

Fig. 4. Results of measurements for duty-cycle of 500 Hz input signal.

The $\chi 2$ test for goodness of fit test was applied to investigate the significance of the differences between observed data in the histograms and the theoretical frequency distribution for data from a normal, uniform or exponential population. If S < $\chi 2$ max, where S is the sum of deviations between the dataset and the assumed distribution, and $\chi 2$ max is the maximum possible allowable deviation in the $\chi 2$ distribution, the hypothesis of appropriate distribution can be accepted [20]. The $\chi 2$ test has been used at 95 % confidence and the number of intervals grouping of experimental data for histograms were from 3 to 6 [23].

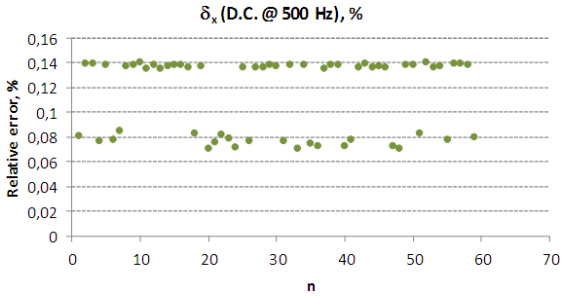

Fig. 5. Relative errors for duty-cycle measurements of 500 Hz input signal.

Table 2. Statistical characteristics of duty-cycle *D.C.* measurements at 100 kHz and 500 Hz input signal.

Parameter	100 kHz	500 Hz
Number of measurements, n	60	60
Minimal *D.C.*, (min)	0.4975	0.5004
Maximal *D.C.*, (max)	0.5129	0.5007
Sampling Range, *D.C.*, (max) - (min)	0.0154	0.0004
Median *D.C.*	0	0
Arithmetic Mean, *D.C.*	0.5049	0.50055
Variance *D.C.*	2.4E-0005	2.3E-0008
Standard Deviation *D.C.*	0.0049	0.0002
Coefficient of Variation *D.C.*	102.7083	3334.0845
Confidence Interval at probability P=95 %	*D.C.*∈ [0.5037 ÷ 0.5061]	*D.C.* ∈ [0.5005 ÷ 0.5006]
Maximal Relative Error, δ_x %	≤ ±1.00	≤ ±0.08
Distribution low:	S < > χ^2	
- uniform	S=7.67 < χ^2 =12 (accepted)	S=117.8> $\chi^2$11 (rejected)
- normal	S=23,69 > χ^2=9.4 (rejected)	S= 162.34 > χ^2 =7.8 (rejected)
- exponential	S=4480.89 > χ^2= 11 (rejected)	S= 53066871 > χ^2= 9.4 (rejected)

As it is visible from the Table 1, the relative error is changed from ±0.08 to ±1.00 % in all specified

measuring range of USTI-MOB at duty-cycle measurements. Such metrological characteristics are very well suitable for many sensors applications.

5. Cases Study

5.1 Low Power Consumption Temperature Sensor System

According to a new market research report 'Temperature Sensor Market, A Study of major Sensor types (ICs, Thermostat, Thermistor, Resistive Temperature Detectors (RTDs), Thermocouple) & Applications, Global Forecast & Analysis 2011 – 2016', the market size of temperature sensors in the year 2010 was $3.27 billion and is expected to reach $4.51 billion units by 2016, at an estimated CAGR of 5.6 % and $6.05 billion by 2020, growing at a CAGR of 5.11 % between 2014 and 2020 [24].

Temperature sensor utilizes digital technology, which means better in efficiency and sensing performance. Temperature sensors have a significant place in different industry verticals. The major applications of temperature sensors are in petrochemical industry, automotive industry, consumer electronics industry, metal industries, food and beverages industry, and healthcare. The emerging applications of temperature sensor in aerospace and defense industry such as temperature stabilization in satellites and Heat Ventilation Automation and Control (HVAC), have fueled the growth of this market [24].

The demand for reliable, high performance and low cost sensors is increasing leading to the development of microtechnology and nanotechnology, offering opportunities like miniaturization, low power consumption, mass production, etc.

The designed low power consumption temperature sensor systems consists of two duty-cycle output sensors SMT16030 (Fig. 6) or SMT172 from *Smartec* [3, 4] and USTI-MOB IC controlled by a microcontroller (in case of sensor systems or smart, digital sensors) or by PC (in case of DAQ systems), Fig. 7.

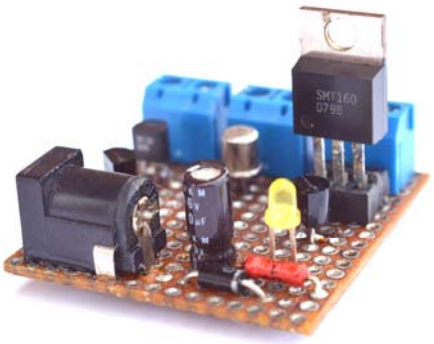

Fig. 6. Temperature sensors SMT16030 from *Smartec* (The Netherlands) on investigation board.

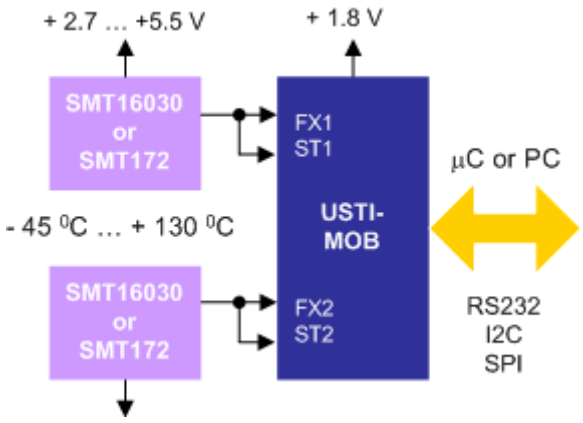

Fig. 7. Low power consumption temperature sensor systems.

These temperature sensors are silicon sensors with duty-cycle outputs with linear responses to temperatures -45 ^{0}C ... + 130 ^{0}C. In applications where multiple sensors are used (more than two), easy multiplexing can be obtained by using a low cost digital multiplexers. The USTI-MOB can work also in so-called master communication mode. In this case no any external microcontroller or PC are necessary. The measuring mode can be selected by the external jumpers, and the USTI-MOD IC continuously forms result of measurement on its RS232 bus at 2800 baud rate.

The temperature sensor SMT160-30 has duty-cycle changes in an output signal from 10.85 % to 93 % at 1-4 kHz [3] (Fig. 8).

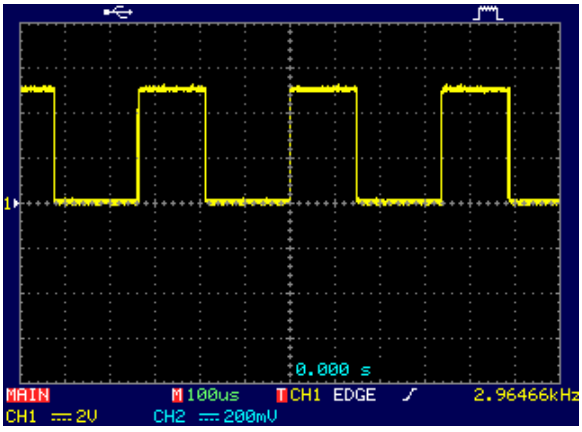

Fig. 8. Temperature sensor SMT16030's output at 24.4 ^{0}C: 44.21 % duty-cycle, 2 964.66 Hz at V_{cc}=4.97 V.

The sensor SMT172 has the same range of duty-cycle but at 0.5 - 7 kHz (the frequency range is the same as in SMT16030 sensor for V_{cc} = 4.7-5.5 V) [4]. The highest frequency in both sensors is achieved at lower supply voltage and in the middle of temperature range.

In general, the duty cycle of the both output sensors' signals is defined by a linear equation [3, 4]:

$$D.C. = 0.320 + 0.00470 \times t, \quad (6)$$

where t is the temperature in ^{0}C. Temperature is then derived from the measured duty cycle.

The maximal total accuracy of SMT16030 temperature sensor in TO220 package and in the temperature range from -45 ^{0}C to +130 ^{0}C is ±1.7 ^{0}C. It means, that the duty-cycle on sensor's output can be changed from 0.4347 (absolute error Δt = *0*) to 0.4428 (absolute error Δt =±1.7 ^{0}C) at +24.4 ^{0}C, for example:

$$D.C. = 0.320 + 0.0047 \times 24.4 = 0.4347$$

$$D.C. = 0.320 + 0.0047 \times (24.4 + 1.7) = \quad (7)$$
$$= 0.4428$$

The relative error for D.C measurement can be calculated as:

$$\delta_{D.C.} = \pm \frac{\Delta D.C.}{D.C.} =$$
$$= \pm \frac{0.4428 - 0.4347}{0.4347} \times 100\,\% = \quad (8)$$
$$= \pm \frac{0.0081}{0.4347} \times 100\,\% = \pm 1.86\,\%$$

The average, total relative error of USTI-MOB at duty-cycle measurement for +24.4 ^{0}C obtained from the experimental investigation is δ_{IC} = ± 0.149 % (Fig. 9 and Fig. 10). The USTI-MOB has been preliminary calibrated at the same temperature and 48 % RH in order to eliminate the quartz crystal's systematic error and short time temperature instability. The small positive trends (dashed lines) observed in both of cases are due to so-called sensor's self-heating effect.

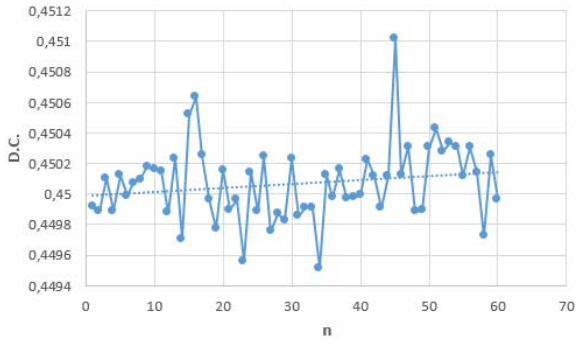

Fig. 9. Duty-cycle values at 60 measurements for the temperature +24.4 ^{0}C.

Taking into account many components of error for temperature sensor's relative error $\delta_{D.C.}$ which is distributed according to the Gaussian distribution low, and the USTI-MOB's relative error δ_{IC} distributed according to the triangular (Simpson's) because of the main component of δ_{IC} is the quantization error, the total mean root square error of temperature sensor system can be calculate as [25, 26]:

$$\sigma_{syst} = \sqrt{\sigma_{D.C.}{}^2 + \sigma_{IC}{}^2} = \sqrt{\left(\frac{\delta_{D.C.}}{2.3}\right)^2 + \left(\frac{\delta_{IC}}{\sqrt{6}}\right)^2} \approx \quad (9)$$
$$\approx \sqrt{0.81^2 + 0.061^2} \approx \pm 0.82\,\%$$

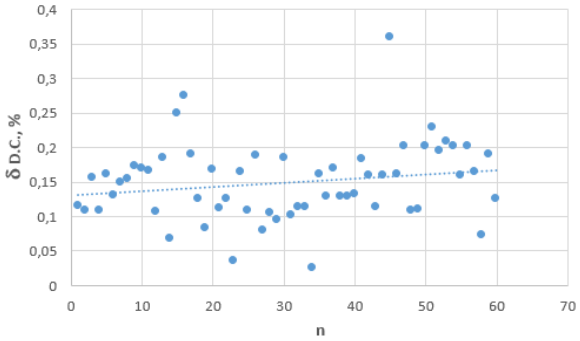

Fig. 10. The relative error of duty-cycle measurement.

In practice, the relative error is more convenient in comparison with the mean root square error, so, it is expediently to calculate the following:

$$\delta_{syst} = \sigma_{syst} \times 2.3 \approx 0.82 \times 2.3 \approx 1.89\,\% \quad (10)$$

Clear, the error's component δ_{IC} can be neglected in comparison with the $\delta_{D.C.}$ component, because of the δ_{IC} is in one order (and even more) less than $\delta_{D.C.}$ [23]. So, in this case the error of the temperature sensor system δ_{syst} is determinated only by the sensor's error itself, and USTI-MOB does not introduce the significant error into the measuring channel.

In order to increase the accuracy, the temperature sensor in TO18, HEC or SOIC-8 packages should be used [3].

The new temperature sensor SMT172 from *Smatrec* has the maximal absolute error for TO-18 package ±0.8 ^{0}C in the same temperature range from -45 ^{0}C to +130 ^{0}C (for other packages the absolute error will be ±1.0 ^{0}C) [4]. In this case the relative error calculated by the same manner as in (8) will be ± 0.87 %.

In order to decrease the absolute error to ±0.1 ^{0}C the following second order equation must be used [4]:

$$T = -2.42 \times D.C.^2 + 215.63 \times D.C. - 68.83 \quad (9)$$

In this case it is recommended to use the USTI IC [18] for accurate duty-cycle measurement instead of

the USTI-MOB IC. The USTI has also the extended rage of frequencies at D.C. measurements (up to 625 kHz), but the increased power consumption (11 mA in comparison with 0.35 mA in the active mode).

5.2 Accelerometers

Dual axis, low cost accelerometer fabricated on a monolithic CMOS IC MXD2125 (*MEMSIC)* provides two outputs that are set to 50% duty cycle at zero *g* acceleration [27]. It measures acceleration with a full-scale range of ±2 g and a sensitivity of 12.5 %/g. It can measure both dynamic acceleration (e.g. vibration) and static acceleration (e.g. gravity). The duty-cycle outputs are proportional to acceleration:

$$A(g) = \frac{(t_p / T_x) - 0.5}{20\ \%} \quad (10)$$

This device is offered from the factory programmed to either a 10 ms period (100 Hz) or a 2.5 ms period (400 Hz).

The sensor can be directly interfaced to the USTI-MOB IC. The accelerometer sensor systems is shown in Fig. 11.

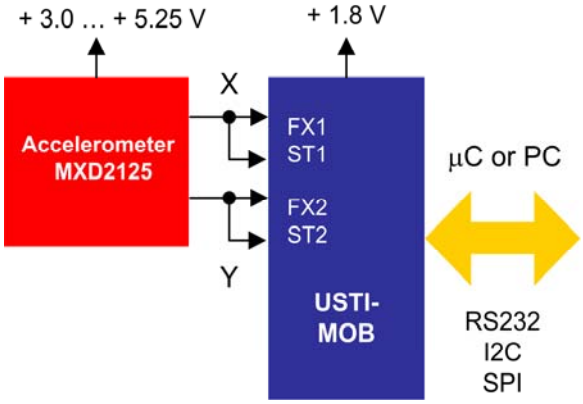

Fig. 11. Accelerometer sensor systems.

Taking into account the low frequency output signal, the USTI-MOB can measure duty-cycles in its two channels with low relative error: < ±0.08 %, which can be neglected in comparison with the accelerometer's error.

The dual axis accelerometers MXD2020E, MXD6025 and MXD6125 (*MEMSIC*); and ADXL202, ADXL210, ADXL212 and ADXL213 (*Analog Devices*) can be also connected to the USTI-MOB by the same way, as it is shown in Fig. 8. The appropriate equations to calculate acceleration from duty-cycle for accelerometers from *Analog Devices, Inc.* are shown in Table. 3.

Table 3. Equations for acceleration calculation.

Accelerometer	Equation	Ref.
ADXL202	$A(g) = \frac{(t_p / T_x) - 0.5}{12.5\ \%}$	[28]
ADXL210	$A(g) = \frac{(t_p / T_x) - 0.5}{4\ \%}$	[29]
ADXL212	$A(g) = \frac{(t_p / T_x) - 0.5}{12.5\ \%}$	[30]
ADXL213	$A(g) = \frac{(t_p / T_x) - 0.5}{30\ \%}$	[31]

Selectable bandwidths for these accelerometer let to use a reasonable frequency for application with the USTI-MOB.

6. Conclusions

The experimental investigation of the designed USTI-MOB integrated circuit working in the duty-cycle and duty-off factor measuring modes confirms its high metrological characteristics at low power consumption (0.35 mA current consumption at V_{cc} = 1.8 V). The relative error of duty-cycle – to – code conversion is changed from ±0.08 to ±1.00 % in all specified measuring range of USTI-MOB at duty-cycle measurements. Metrological performances (relative error and frequency range) can be improved in four times if to use the USTI IC [1, 19] instead of the USTI-MOB, if the power consumption is not a critical parameter at the design.

The optimal trade-off between accuracy, power consumption and communication speed has achieved. It makes the USTI-MOB suitable for application in various duty-cycle output sensors such as temperature sensors, accelerometers, magnetic sensors, Hall Effect gear tooth sensors etc. to produce smart, digital output sensors, DAQ systems or sensor systems. The significant time-to-market reduction will be achieved in such design approach.

The USTI-MOB IC will be introduced on the modern market at the end of 2015 by *Technology Assistance BCNA 2010, S .L. (Excelera),* Barcelona, Spain (http://www.excelera.io).

References

[1]. S. Y. Yurish, Digital Sensors and Sensor Systems: Practical Design, *IFSA Publishing*, 2011.
[2]. Sensors Web Portal (http://www.sensorsportal.com).
[3]. SMT16030 Digital Temperature Sensor, Datasheet, *Smartec*, March 2015.
[4]. SMT172, Datasheet, *Smartec*, June 2015.

[5]. G. de Graaf, R. F. Wolffenbuttel, Light-to-Frequency Converter Using Integrated Mode Photodiodes, in *Proceedings of IMTC'96*, 4-6 June, 1996, Brussels, Belgium, pp.1072-1075.

[6]. D. Hernandez, R. Amador, I. León, K. Kohlhof, Constant temperature anemometer with duty-cycle output conversion, in *Proceedings of the IX Workshop IBERCHIP 2003*, Habana, Cuba, March 2003.

[7]. Gerard C. M. Meijer, Concepts and Focus Point for Intelligent Sensor Systems, *Sensors and Actuators A*, Vol. 41-42, 1994, pp.183-191.

[8]. S. Middelhoek, P. J. French, J. H. Huijsing and W. J. Lian, Sensors with Digital or Frequency Output, *Sensors and Actuators*, Vol. 15, 1988, pp. 119-133.

[9]. V. Ferrari , A. Ghisla, Zs. Kovács Vajna, D. Marioli, A. Taroni, ASIC front-end interface with frequency and duty cycle output for resistive-bridge sensors, *Sensors and Actuators A*, Vol. 138, 2007, pp. 112–119.

[10]. Zeljko Ignjatovic, Mark F. Bocko, An Interface Circuit for Measuring Capacitance Changes Based Upon Capacitance-to-Duty Cycle (CDC) Converter, *IEEE Sensors Journal*, Vol. 5, No. 3, June 2005, pp. 403-410.

[11]. J. Cañete, S. Y. Yurish, Sensors Systems for Smartphones, Tablets and IoT: New Advanced Design Approach, *Sensors & Transducers*, Vol. 187, Issue 4, April 2015, pp. 1-9.

[12]. P. C. de Jong and F. N. Toth, Measuring Duty Cycles with an Intel MCS-51 Microcontroller, Available online at http://www.smartec.nl/pdf/appsmt01.pdf

[13]. J. Bauer, Various Solutions for Calculating a Pulse and Duty Cycle, AN1473, *Microchip Technology, Inc.*, 2012.

[14]. J. Vuori, Simple Method Measures Duty Cycle, *EDN Magazine*, March 3, 1997.

[15]. G. Chao, G. C. M. Meijer, A Novel Method of Reading the Time-Domain Sensor Signals, in *Proceedings of ProRISC*, November 29-30, 2001, Veldhoven, The Netherlands.

[16]. S. S. Huang and M. S. Young, Method for Designing a Temperature Measurement System Using Two Phase-locked Loops, *Review of Scientific Instruments*, Vol. 74, No. 8, August 2003, pp. 3826 - 3831.

[17]. Eric Jacobsen, Designing a Homemade Digital Output for Analog Voltage Output Sensors, Application Note AN1586, *Freescale Semiconductor*, 2006.

[18]. S. Y. Yurish and J. Cañete, Universal Sensors and Transducers Interface for Mobile Devices: Metrological Characteristics, *Sensors & Transducers*, Vol. 188, Issue 5, May 2015, pp. 15-25.

[19]. Universal Sensors and Transducers Interface (USTI), Specification and Application Note, *Technology Assistance BCNA 2010, S. L. (Excelera)*, 2010.

[20]. E. Schrufer, Signal Processing: Digital Signal Processing of Discrete Signals, *Lybid'*, Kiev, 1992, (in Ukrainian).

[21]. 33500B Series Waveform Generators, Data Sheet, *Agilent Technologies, Inc.*, USA, 2012.

[22]. Agilent 53200A Series RF/Universal Frequency Counter/Timers, Data Sheet, *Agilent Technologies, Inc.*, USA, 2010.

[23]. P. V. Novitskiy, I. A. Zograf, Errors Estimation for Measuring Results, *Energoatomizdat*, Leningrad, 1991 (in Russian).

[24]. Global Temperature Sensor Market worth $4.51 Billion by 2016, *MarketsandMarkets*, November 2014.

[25]. N. V. Kirianaki, S. Y. Yurish, N. O. Shpak, V. P. Deynega, Data Acquisition and Signal Processing for Smart Sensors, *John Wiley & Sons*, UK, Chichester, 2001.

[26]. Sergey Y Yurish, Ferran Reverter, Ramon Pallas-Areny, Measurement error analysis and uncertainty reduction for period- and time-interval-to-digital converters based on microcontrollers, *Measurement Science and Technology*, 16, 2005, pp. 1660–1666.

[27]. Improved, Ultra Low Noise ±2g Dual Axis Accelerometer with Digital Outputs, MXD2125GL/HL, MXD2125ML/NL, *MEMSIC, Inc.*, USA, 2004.

[28]. Low Cost 62 g/610 g Dual Axis iMEMS® Accelerometers with Digital Output, ADXL202/ADXL210, Rev. B, *Analog Devices, Inc.*, 1999.

[29]. Dual-axis Accelerometer Evaluation Board ADXL210EB, *Analog Devices, Inc.*, USA, 2003.

[30]. Precision ±2 g Dual Axis, PWM Output Accelerometer ADXL212, *Analog Devices, Inc.*, 2011.

[31]. Low Cost ±1.2 g Dual Axis Accelerometer ADXL213, Rev. A, *Analog Devices, Inc.*, 2010.
